Electronic Supplementary Material (ESI) for Nanoscale Horizons.
This journal is © The Royal Society of Chemistry 2019

Supporting Information

for

Dimension conversion: from 1D metal-organic gel into 3D metal-organic porous network with high-efficiency multiple enzyme-like activities for cascade reaction

Zhong Wei Jiang, Ting Ting Zhao, Yuan Fang Li and Cheng Zhi Huang**

1. Experimental Section

1.1 Reagents and apparatus

All chemicals and reagents were of analytical grade and used without further purification. 4,4′,4″-s-triazine-1,3,5-triyltri-p-aminobenzoate (H_3TATAB) was purchased from Na Qian Chemistry Co., Ltd. (Shanghai, China). Terephthalic acid (TPA) and o-phenylenediamine (OPD) were obtained from Aladdin Chemistry Co., Ltd. (Shanghai, China). Cupric (II) chloride dihydrate ($CuCl_2 \cdot 2H_2O$) was obtained from Tianjin Hygain Chemical (Group) Co., Ltd (Tianjin, China). Cysteine (Cys), glucose (Glc), glutathione (GSH), and 30% (v/v) H_2O_2 were purchased from Sinopharm Chemical Reagent Co. Ltd. (Shanghai, China). Proline (Pro), aspartic acid (Asp), threonine (Thr), tryptophan (Trp), phenylalanine (Phe), Galactose (Gal), isoleucine (Ile), methionine (Met), citric acid (CA), uric acid (UA), arginine (Arg), alanine (Ala), leucine (Leu), histidine (His) and homocysteine (Hcy) were purchased from Aladdin Chemistry Co. Ltd. (Shanghai, China). Human serum albumin (HSA) and human Cyr61 were purchased from AmyJet Scientific Inc. Ultrapure water (18.2 MΩ) was used throughout the experiment.

An S-4800 scanning electron microscope (SEM) (Hitachi, Japan) was used to imaging the morphology of Cu-MOG and Cu-MOPN. Transmission electron microscopic (TEM) characterization was performed on JEOL JEM-1200EX TEM instrument (JEOL, Japan). The xerogels were obtained by a Cool safe 110–4 freeze-drying apparatus (Labogene, Denmark). Powder X-ray diffraction (PXRD) patterns were collected on a D8ADVANCE X-ray

diffractometer (Bruker, Germany) with Cu Kα radiation (λ = 1.5406 Å) at a scan rate of 3.00° min^{-1}. X-ray photoelectron spectrometry (XPS) analyses were carried out on a Thermo Escalab 250Xi X-ray photoelectron spectrometer using an Al Kα source (hν =1486.6 eV). The infrared spectra of the materials were recorded by an IR Prestige-21 (Shimadzu, Japan) instrument in the range of 500−3500 cm^{-1} using the KBr pellet technique. The BET surface area was determined by N_2 adsorption–desorption isotherms obtained at 77 K on ASAP 2020, USA. Thermogravimetry analysis (TGA) was conducted on a Q600 (TA Instruments, USA) thermogravimetric analyzer. F-2500 fluorescence spectrophotometer (Hitachi, Tokyo, Japan) was used for fluorescence measurement. F-4600 fluorescence spectrophotometer (Hitachi, Tokyo, Japan) was used for kinetic measurment.

1.2 Synthesis of Cu-MOG and Cu-MOPN

Synthesis of Cu-MOG: typically, 200 mg (0.46 mmol) of H_3TATAB was dissolved in 10 mL ultrapure water (containing 200 μL triethylamine (TEA)) to prepare stock solution. The stock solution of Cu^{2+} were prepared by dissolving $CuCl_2 \cdot 2H_2O$ (0.46 mmol, 79 mg) in 10 mL ultrapure water. For the synthesis of Cu-MOG, 500 μL of Cu^{2+} solution was simply mixed with equal volume H_3TATAB. After standing 15 min at room temperature, the Cu-MOG were obtained. Then, the Cu-MOG were further washed three times with DMF and redispersed in DMF.

Synthesis of Cu-MOPN: the obtained Cu-MOG dispersion solution was added into a 3 mL Pyrex vial. After that, the capped vials were heated for 30 minutes under microwave irradiation in a household microwave oven (M1-L213B, Midea Co., Ltd., China) with medium low power (about 231W). After cooling down to room temperature, the resulting Cu-MOPN was washed three times with ethanol, and then collected by centrifugation at 10,000 r.p.m for 3 min. Finally, the obtained Cu-MOPN was dried in a vacuum oven at 60 °C for further use.

Compared with microwave reactor, household microwave oven is small and cheap. Unfortunately, household microwave ovens do not have temperature controllers like microwave

reactors. So, we can only regulate the reaction conditions by optimizing different microwave power. There are five microwave power levels: low power (about 119W), medium low power (about 231W), medium power (about 385W), medium high power (about 539W) and high power (about 700W). We have tried to prepare Cu-MOPN by using different microwave power. However, low power (about 119W) cannot effectively convert Cu-MOG to Cu-MOPN, and the solvent would evaporate greatly by applying medium power (about 385W). The Cu-MOG can be effectively converted to Cu-MOPN by applying medium low power (about 231W). Therefore, we chose medium low power (about 231W) as optimal microwave power.

Stability of Cu-MOPN and Cu-MOG: The as-prepared Cu-MOPN and Cu-MOG were placed in hydrochloric acid with pH= 2 and sodium hydroxide with pH=12, respectively. After soaking 6 hours, the obtained Cu-MOPN and Cu-MOG were characterized by SEM, XRD and N_2 adsorption–desorption measurement.

Raman spectrum measurrment: The supernatant of Cu-MOPN+ cysteine before and after reaction was mixed with Ag NPs (about 50 nm), respectively. After standing 5 min, the Raman spectrometer (HR800) was used to collect Raman spectrum.

1.3 The oxidase- and peroxidase-like activity of Cu-MOG and Cu-MOPN

In this work, the same mass concentration of Cu-MOPN and Cu-MOG was used. Since Cu-MOPN is obtained by *in situ* conversion of Cu-MOG under microwave stimulation. Therefore, we believe that they have the same composition. Besides, the significant difference between Cu-MOPN and Cu-MOG is the morphology. Different morphologies lead to different BET surface area and hierarchical porous structure. Hence, we believe that the difference of BET surface area and hierarchical porous structure are the key factors leading to different catalytic activities.

The oxidase- like activity: For investigating the oxidase-like activity of the as-prepared Cu-MOG and Cu-MOPN, a fluorometric strategy was performed via a catalytic reaction towards the oxidation of OPD. Typically, 50 μL of OPD (1mM) and 50 μL of Cu-MOG (200 μg/mL)

or Cu-MOPN (200 μg/mL) solution were added into 300 μL of PB (200 mM, pH 7.25) buffer solution and finally diluted to 500 μL by using ultrapure water. After incubating at 70 °C for 30 min, the resulting reaction solution was measured by using F-2500 fluorescence spectrometer under the excitation wavelength of 425 nm and detecting the emission intensity at 573 nm.

The peroxidase-like activity: The TPA as a fluorescent probe for hydroxyl radical was used to investigate the peroxidase-like activity of the as-prepared Cu-MOG and Cu-MOPN. Herein, Cu-MOG (200 μg/mL, 50 μL) or Cu-MOPN (200 μg/mL, 50 μL), TPA (20 mM, 50 μL) and H_2O_2 (100μM, 100μL) were orderly added into 300 μL of phosphate buffer (200 mM, pH 7.25). After incubating at 45 °C for 20 min, fluorescence spectra were measured under the excitation wavelength of 315 nm.

Cascade reaction for Cys determination: 50 μL of TA (20 mM) and 50 μL of Cu-MOPN (200 μg/mL) and 50 μL cysteine solution with different concentrations were orderly added into 300 μL of PB (200 mM, pH 7.25) buffer solution and further diluted to 500 μL by using ultrapure water. After incubating at 70 °C for 20 min, fluorescence spectra were measured under the excitation wavelength of 315 nm.

Selective experiment: 50 μL of TA (20 mM) and 50 μL of Cu-MOPN (200 μg/mL), 50 μL cysteine (200 μM) or 50 μL interferent (2 mM, especially, 0.24g/L for HSA and Cyr 61) were orderly added into 300 μL of PB (200 mM, pH 7.25) buffer solution and further diluted to 500 μL by using ultrapure water. After incubating at 70 °C for 20 min, fluorescence spectra were measured under the excitation wavelength of 315 nm.

Detection of Cys in serum: First, human plasma samples were pretreated by ultrafiltration to eliminate the possible interference of proteins, and then the eluents were used instead of cysteine solution for cascade reaction.

Steady-State kinetic analysis of the cascade reaction system: Kinetic assays were performed with varied Cys concentrations under optimal conditions. To calculate the initial rate, the

standard curve of TAOH has been tested. The apparent maximum initial velocity (V_{max}) and Michiaelis-Menten constant (K_m) were calculated by Lineweaver-Burk plots.

2. Figures

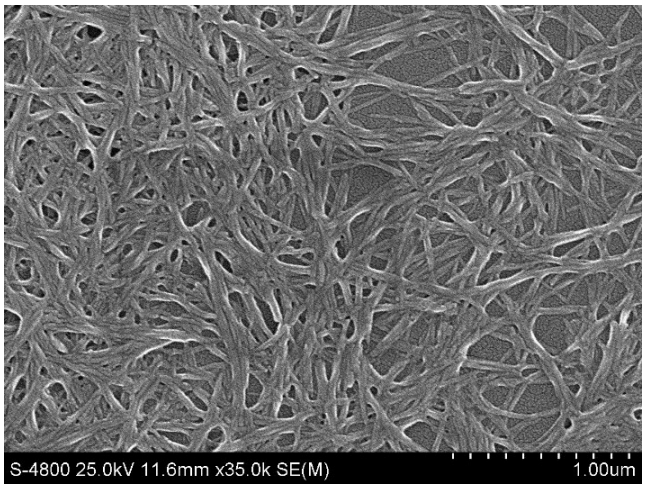

Fig. S1 The SEM image of Cu-MOG.

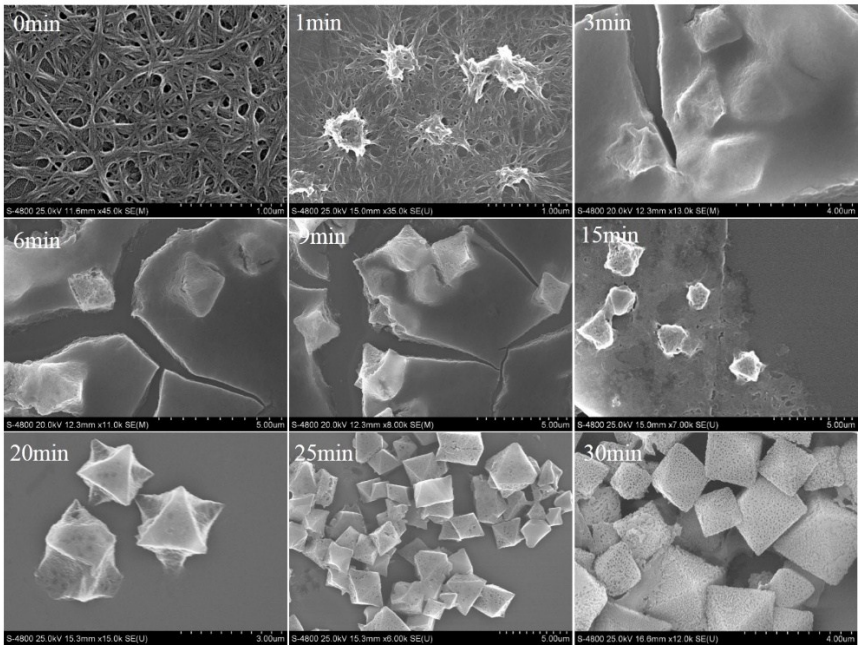

Fig. S2. The SEM images of Cu-MOPN at different reaction time.

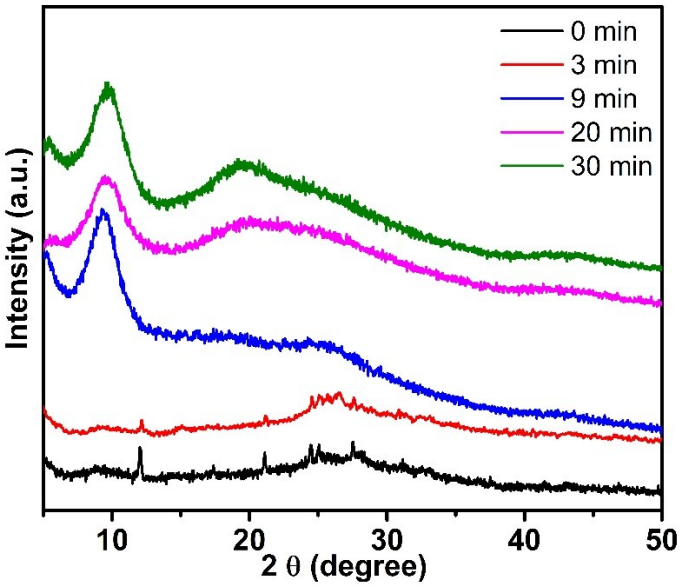

Fig. S3 The PXRD patterns of Cu-MOPN at different reaction time.

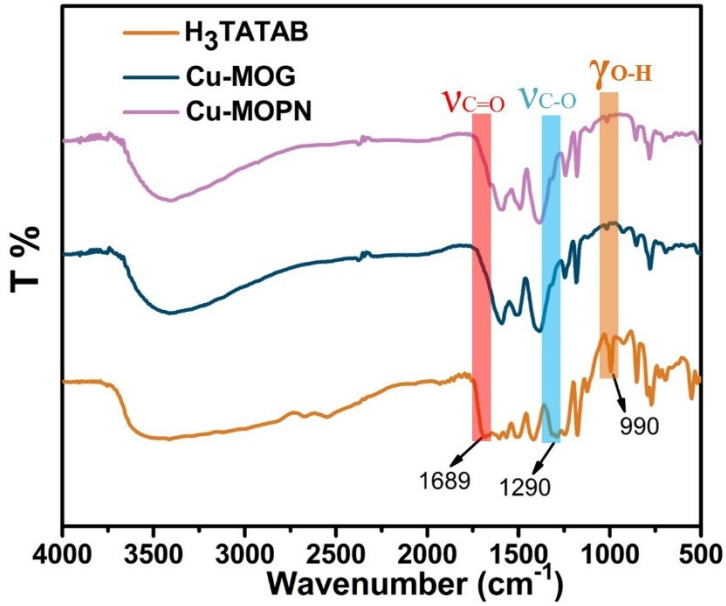

Fig. S4 The FT-IR spectra of free H_3TATAB, Cu-MOG and Cu-MOPN

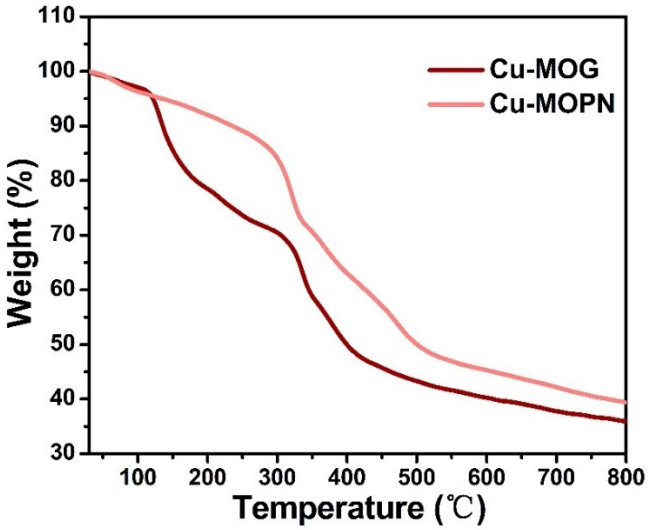

Fig. S5 TGA curves of Cu-MOG and Cu-MOPN measured in N_2 atmosphere at a temperature ramp of 10 ^{o}C min^{-1}.

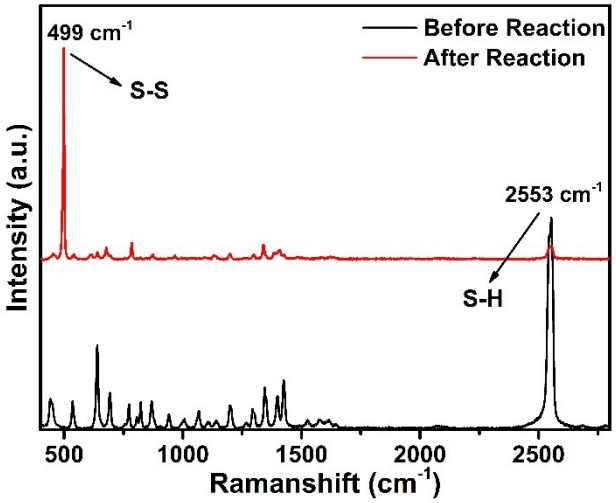

Fig. S6 The Raman spectra of cysteine before and after the reaction.

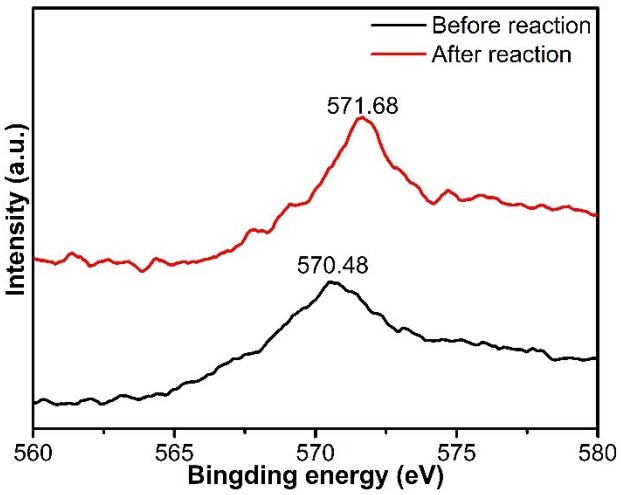

Fig. S7 The corresponding Cu LMM Auger spectra before and after treat with cysteine.

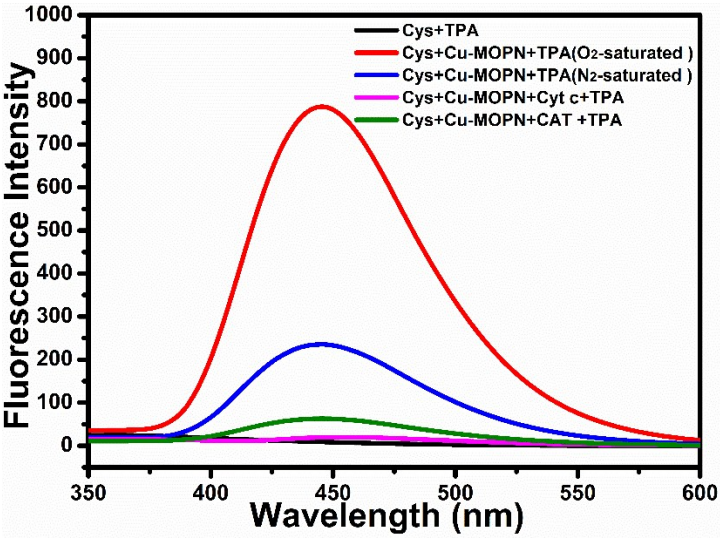

Fig. S8 Fluorescence spectra of different reaction systems.

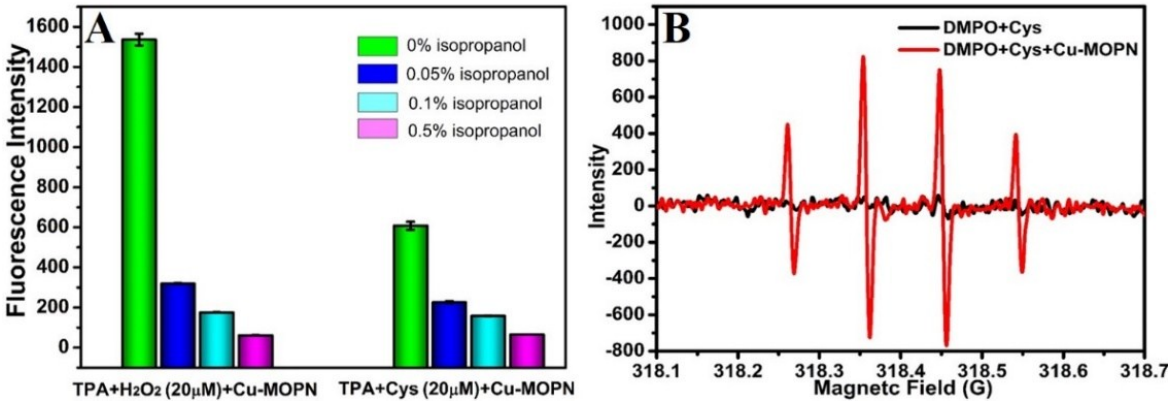

Fig. S9 Catalytic oxidation of TPA in TPA+H_2O_2+Cu-MOPN and TPA+Cys+Cu-MOPN reaction system with the presence of different isopropanol concentration (A), and the ESR spectra for different systems (B).

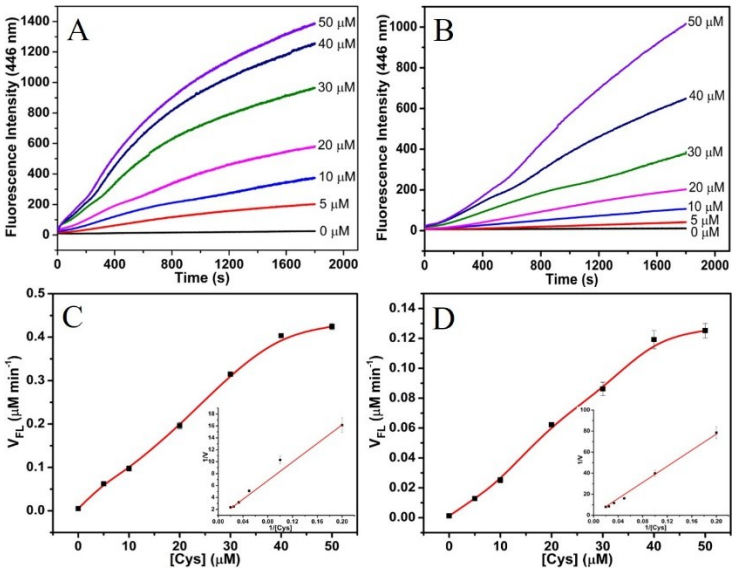

Fig. S10 Time-dependent fluorescence changes of TAOH in the presence of variable concentrations of Cys in Cu-MOPN (A) and Cu-MOG (B)catalytic system, and the corresponding steady-state kinetic analysis using Michaelis−Menten model (C and D). Inset: Lineweaver−Burk double reciprocal plot.

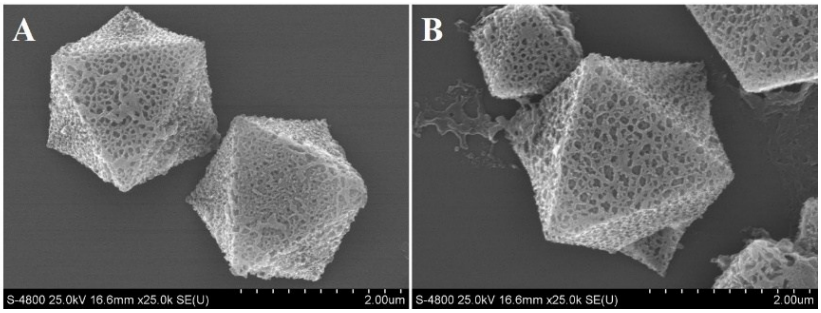

Fig. S11 The SEM images of Cu-MOPN after treatment with HCl (pH=2) (A) and NaOH (pH=12) (B).

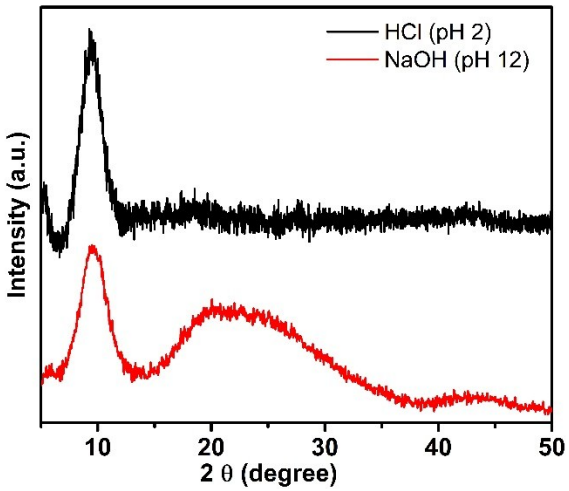

Fig. S12 The PXRD pattern of Cu-MOPN after treatment with HCl and NaOH.

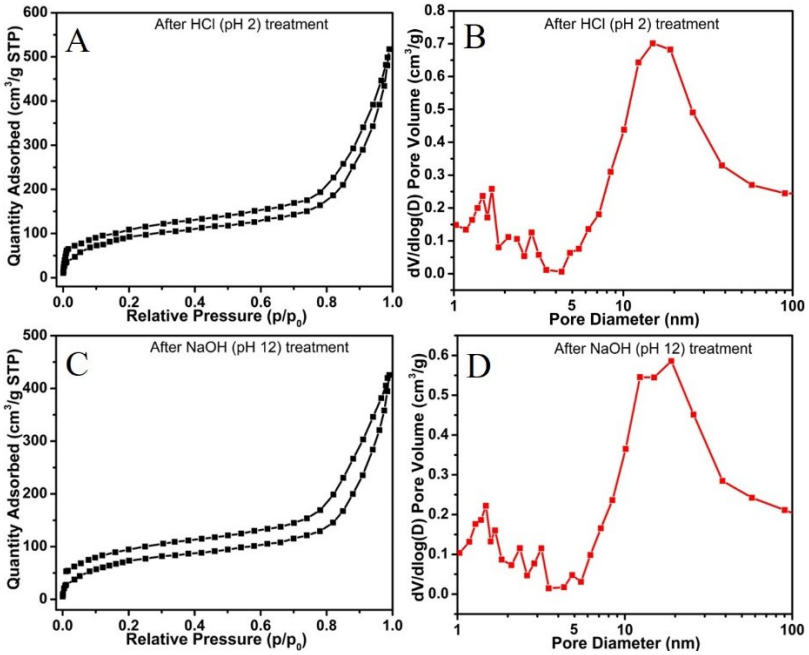

Fig. S13 The N_2 adsorption-desorption isotherms of Cu-MOPN after treatment with HCl (A) and NaOH (C), and the corresponding pore size curve distribution (B and D).

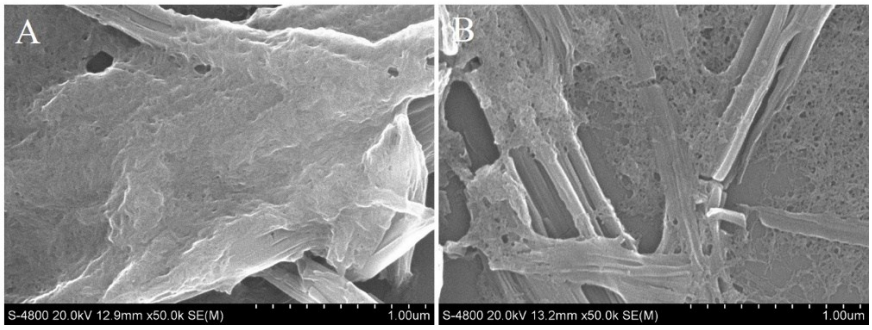

Fig. S14 The SEM images of Cu-MOG after treatment with HCl (pH=2) (A) and NaOH (pH=12) (B).

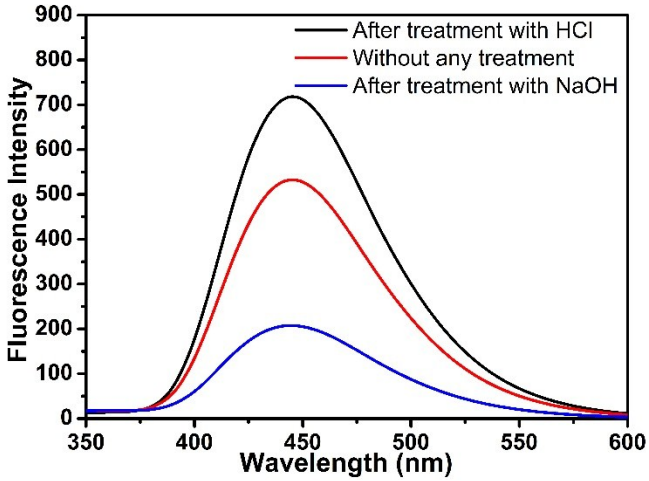

Fig. S15 The fluorescence spectra of cascade reaction of Cu-MOPN after treatment with HCl and NaOH.

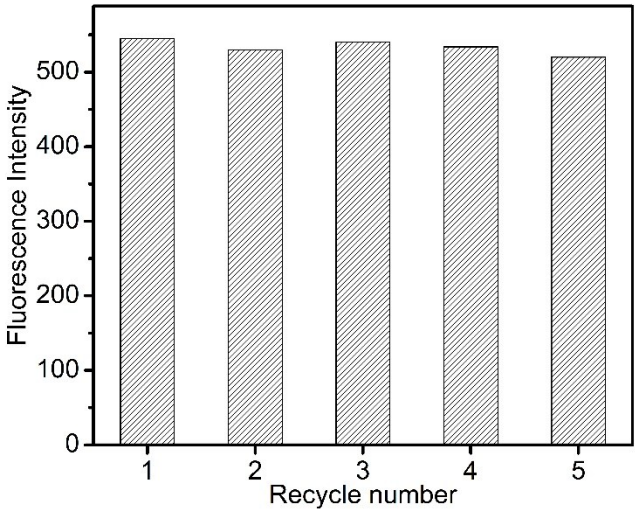

Fig. S16 The recyclability of the cascade reaction system after five consecutive reaction.

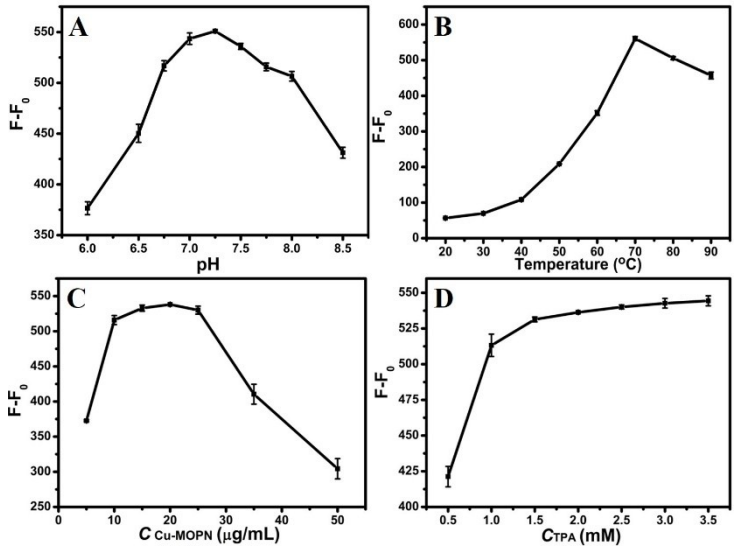

Fig. S17 The optimization of experimental conditions. (A) pH, (B) reaction temperature, (C) Cu-MOPN concentration, (D) TPA concentration.

Table S1 Kinetic Parameters of Cu-MOPN and Cu-MOG.

Catalyst	Substrate	K_m [mM]	V_{max} [μM min^{-1}]
Cu-MOPN	Cys	0.13	1.72
Cu-MOG	Cys	0.21	0.71

Table S2 The recovery test of cysteine in diluted serum samples.

Serum samples	Added (μM)	Detected (mean, μM)	RSD (n=3, %)	Recovery (%)
1	0	2.85	0.2	-
	2	4.76	1.1	95.5
	4	6.81	0.9	99.0
2	0	3.06	0.6	-
	2	5.11	1.4	102.5
	4	7.22	1.9	104.0

Table S3. The analytical comparison for determination of cysteine between this work and other works.

Materials	Method	Liner range	LOD	Interference	Ref.
$CuMnO_2$	Colorimetry	25−300 μM	11.26 μM	—	1
$BaTiO_3$	Electrochemistry	10−1000 μM	10 μM	None	2
N-GQD@V_2O_5	Fluorimetry	0.1−125 μM	50 nM	None	3
UiO-MOF	Fluorimetry	10^{-11}−10^{-3} M	10^{-11} M	GSH	4
Amino nitrogen quantum dots	Fluorimetry	0.3−3.0 μM	0.1 μM	None	5
G-quadruplex-Cu(II)	Colorimetry	5−500 nM	5 nM	His	6
AgAuNCs@11-MUA	Fluorimetry	0.25−7 μM	111 nM	His	7
Co-CDs	Fluorimetry	0.1−100 μM	80 nM	None	8
CuO−Cu_2O	Photoelectrochemistry	0.2−10 μM	50 nM	Hcy, GSH	9
Cu-MOPN	Fluorimetry	1−50 μM	93 nM	None	**This study**

References

1 Y. Chen, T. Chen, X. Wu and G. Yang, *Sens. Actuators. B. Chem.*, 2019, **279**, 374-384.
2 S. Selvarajan, N. R. Alluri, A. Chandrasekhar and S.-J. Kim, *Biosens. Bioelectron.*, 2017, **91**, 203-210.
3 A. B. Ganganboina, A. Dutta Chowdhury and R. A. Doong, *ACS Appl. Mater. Interfaces*, 2018, **10**, 614-624.
4 Y. A. Li, C. W. Zhao, N. X. Zhu, Q. K. Liu, G. J. Chen, J. B. Liu, X. D. Zhao, J. P. Ma, S. Zhang and Y. B. Dong, *Chem. Commun.*, 2015, **51**, 17672-17675.
5 Z. Tang, Z. Lin, G. Li and Y. Hu, *Anal. Chem.*, 2017, **89**, 4238-4245.
6 C. Wu, D. Fan, C. Zhou, Y. Liu and E. Wang, *Anal. Chem.*, 2016, **88**, 2899-2903.
7 J. Sun, F. Yang, D. Zhao, C. Chen and X. Yang, *ACS Appl. Mater. Interfaces*, 2015, **7**, 6860-6866.
8 H. Liu, Y. Sun, J. Yang, Y. Hu, R. Yang, Z. Li, L. Qu and Y. Lin, *Sens. Actuators. B. Chem.*, 2019, **280**, 62-68.
9 Y. Zhu, Z. Xu, K. Yan, H. Zhao and J. Zhang, *ACS Appl. Mater. Interfaces*, 2017, **9**, 40452-40460.